Medical Engineering & Physics 36 (2014) 905–914

Contents lists available at ScienceDirect

Medical Engineering & Physics

journal homepage: www.elsevier.com/locate/medengphy

# The influence of an unilateral carotid artery stenosis on brain oxygenation

T. Köppl[a,*], M. Schneider[b], U. Pohl[c], B. Wohlmuth[a]

[a] Institute for Numerical Mathematics, Technische Universität München, Boltzmannstr. 3, D-85748 Garching b. München, Germany
[b] Department of Hydromechanics and Modelling of Hydrosystems, Pfaffenwaldring 61, D-70569 Stuttgart, Germany
[c] Walter-Brendel-Centre of Exp. Medicine, Ludwig-Maximilians-Universität, Marchionistr. 27, D-81377 München, Germany

ARTICLE INFO

*Article history:*
Received 10 December 2013
Received in revised form 24 March 2014
Accepted 31 March 2014

*Keywords:*
Multi-scale model
Stenosis
Circle of Willis
Oxygen supply
Domain decomposition
Transport equations
Model reduction

ABSTRACT

We study the impact of varying degrees of unilateral stenoses of an carotid artery on pulsatile blood flow and oxygen transport from the heart to the brain. For the numerical simulation a model reduction approach is used involving non-linear 1-D transport equation systems, linear 1-D transport equations and 0-D models. The haemodynamic effects of vessels beyond the outflow boundaries of the 1-D models are accounted for using a 0-D lumped three element windkessel model. At the cerebral outflow boundaries the 0-D windkessel model is extended by metabolic autoregulation, based on the cerebral oxygen supply. Additionally lumped parameter models are applied to incorporate the impact of the carotid stenosis. Our model suggests that for a severe unilateral stenosis in the right carotid artery the partial pressure of oxygen in the brain area at risk can only be restored, if the corresponding cerebral resistance is significantly decreased and if the circle of Willis (CoW) is complete.



## 1. Introduction

Despite improvements in primary prevention, the incidence of atherosclerotic vascular lesions and their consequences for organ function and integrity will remain a major medical problem in an aging society [18]. Stenoses in the carotid arteries are relevant causes of brain ischaemia [26] when they become occluded either by an increasing stenosis or, more acutely, by the development of a thrombus. The reduction of blood flow due to a stenosis in one carotid artery can potentially be compensated by blood flow through collateral vessels known as the circle of Willis (CoW) [21] being fed by the contralateral carotid artery [16,20,21,24,34].

There exist many approaches to model this situation mathematically in order to predict the amount of blood flow, that, under a given degree of stenosis, can be supplied by the contralateral carotid artery via the CoW. In order to avoid time consuming 3-D computations, several models are based on reduced 1-D and 0-D lumped parameter models, which can be derived from the incompressible 3-D Navier–Stokes equations and a convection diffusion equation by averaging techniques, see, e.g., [4,6,[8, Chapter 2],10[11, Chapter 10], 28]. Using these reduced and lumped parameter models, different multi-scale models for pulsatile blood flow within arterial networks were developed [2,9,[11, Chapter 11],22,30,31,36]. An analysis on the existence and uniqueness of the solution of these models can be found in Quarteroni et al. [10,23]. The accuracy of a multi-scale model, was investigated, e.g., in Alastruey et al. [1,4]. Within these references, the authors applied this multi-scale model to human arterial trees, consisting of the larger arteries and found a good agreement between the numerical results and medical data. To incorporate the impact of a stenosis, in some publications a 0-D lumped parameter model replaces the stenosis and couples the adjacent reduced models [19,29,32,35].

In this paper, a multi-scale model is presented, in which we interconnect different types of reduced 1-D or 0-D lumped parameter models at the bifurcations of the arterial network. By this, the different features of large and middle sized vessels and also small vessels can be better accounted for. In addition, the coupling of the linearized 1-D models and the 0-D lumped parameter models can be described by linear systems of equations which can be solved with less effort than the non-linear ones. A similar approach was investigated in Cristiano et al. [7], where a 3-D model for the abdominal aorta and a 1-D model for the remaining vessel system are used. To simulate oxygen transport,

* Corresponding author. Tel.: +49 8928918413.
*E-mail addresses:* koeppl@ma.tum.de, tobiaskoeppl@gmx.de (T. Köppl).

http://dx.doi.org/10.1016/j.medengphy.2014.03.020
1350-4533/

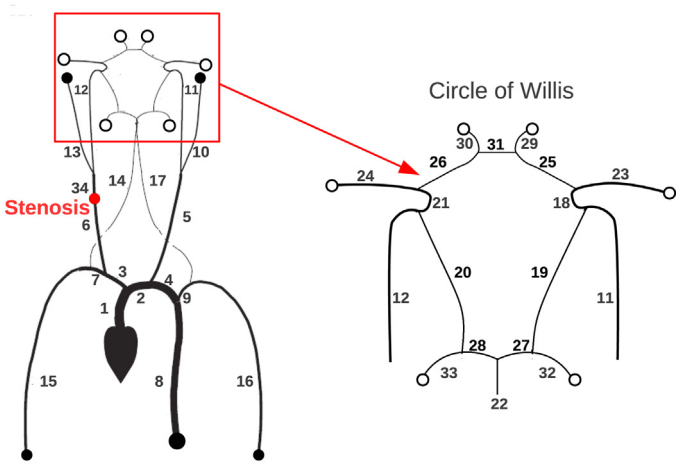


**Fig. 1.** Outflow boundaries marked with an • are coupled with a three element windkessel model having fixed resistances [3]. Resistances at outflows marked with ○ are variable, depending on the partial pressure of oxygen in the brain tissue.

most of the existing models have to be extended by an additional equation and coupling equations at the bifurcations. Furthermore, none of the mentioned models considers the consequences of collateral blood flow for the oxygen supply of brain tissue. We modify and generalize existing models [2] including metabolic cerebral autoregulation, to understand the consequences for mean oxygen tension in brain areas at risk under conditions of varying unilateral stenoses and collateral blood flows.

## 2. Mathematical models

For the simulation of blood flow and oxygen transport from the heart to the brain, we consider the arterial vessel system, presented in Alastruey et al. [2,3].

It consists of 33 arteries, containing the circle of Willis and the most important arteries, branching out of the heart (see Fig. 1). Our numerical scheme is based on a domain decomposition technique, i.e., we split the network into its single vessels and assign in a first step, a decoupled submodel to each vessel. Only in a second step, we interconnect the independent subsystems by suitable transmission conditions. The simulation of blood flow and the oxygen transport within a single vessel is carried out by reduced models. These models have the form of 1-D transport equation systems or 0-D lumped parameter models [3,4,8,9,[11, Chapters 7, 10, 11],19,31,32,37]. Considering the given vessel system, it becomes obvious that this network is composed of arteries having different length scales. Therefore, it is beneficial to use different models taking the special features of the vessels into account. The arteries within or near the CoW exhibit elastic properties which differ considerably from those of the aorta (vessel 1 in Fig. 1). We apply non-linear transport equation systems [2,6] [8, Chapter 2] to the larger vessels $\Omega_i$, numbered by $i \in \{1, \ldots, 9, 15, 16, 34\}$ and linear transport equation systems, incorporating the small displacement property, to the vessels $\Omega_i$, numbered by $i \in \{10, \ldots, 14, 17, \ldots, 26, 29, 30, 32, 33\}$ (see Fig. 1). Due to their small length (below 1 cm) and section area, the blood flow and oxygen transport through the remaining vessels $\Omega_i$ numbered by $i \in \{27, 28, 31\}$ are computed by 0-D lumped parameter models [3,4]. The corresponding subsystems are coupled at the bifurcations by appropriate algebraic constraints. The following subsections describe the characteristic features belonging to our model in more detail. In particular, we outline how the existing models can be extended to simulate the transport of oxygen.

### 2.1. Modeling the blood flow and oxygen transport within a single vessel

The non-linear 1-D transport system for the $i$th vessel $\Omega_i$ having the length $l_i$ and the section area $A_{0,i}$ is given by [3,4][8, Chapter 2]:

$$\frac{\partial A_i}{\partial t} + \frac{\partial Q_i}{\partial z} = 0, \quad z \in (0, l_i),\ t > 0, \tag{1a}$$

$$\frac{\partial Q_i}{\partial t} + \frac{\partial}{\partial z}\left(\frac{Q_i^2}{A_i}\right) + \frac{A_i}{\rho}\frac{\partial p_i}{\partial z} = -K_r \frac{Q_i}{A_i}, \quad z \in (0, l_i),\ t > 0, \tag{1b}$$

$$\frac{\partial \Gamma_i}{\partial t} + \frac{\partial}{\partial z}\left(\frac{\Gamma_i Q_i}{A_i}\right) = 0, \quad z \in (0, l_i),\ t > 0, \tag{1c}$$

where $A_i$, $Q_i$, $\Gamma_i$ and $p_i$ denote the section area, average volumetric flux, averaged concentration and mean pressure of the $i$th vessel, $i \in \{1, \ldots, 33\}$, respectively. By $z$ and $t$, we denote the space and time variable. $\rho$ is the blood density. The coefficient $K_r$ is a resistance parameter linked to the blood viscosity $\eta$: $K_r = 22\pi\eta/\rho$. The main assumptions leading to this specific choice of $K_r$ are provided in Alastruey et al. [4]. If $G_{0,i}$ and $A_{0,i}$ are constant along $z$, a suitable way to close this system is to provide an algebraic relation between the pressure and the vessel area $A_i$:

$$p_i(z,t) = G_{0,i}\left(\sqrt{\frac{A_i}{A_{0,i}}} - 1\right), \quad G_{0,i} = \frac{\sqrt{\pi} h_{0,i} E_i}{\left(1-\nu^2\right)\sqrt{A_{0,i}}}, \tag{2}$$

where $E_i$ is the Young modulus, $h_{0,i}$ is the vessel thickness and $\nu$ is the Poisson ratio. Since biological tissue is practically incompressible, we choose the Poisson ratio: $\nu = 0.5$. The algebraic equation (2) assumes that the vessel wall is instantaneously in equilibrium with the pressure forces acting on it. Further effects like wall inertia and viscoelasticity could be incorporated, by the help of a differential pressure law, presented e.g. in Alastruey et al. [5] and Formaggia et al. [11, Chapter 10].

An analysis of the characteristics of the system (1a), (1b), (1c) and (2), reveals that changes in pressure, flow rate and concentration are propagated by $W_{1,i}$, $W_{2,i}$ and $W_{3,i}$ [8, Chapter 2]:

$$W_{1,i} = -\frac{Q_i}{A_i} + 4\sqrt{\frac{G_{0,i}}{2\rho}}\left(\frac{A_i}{A_{0,i}}\right)^{1/4}, \quad W_{2,i} = \frac{Q_i}{A_i} + 4\sqrt{\frac{G_{0,i}}{2\rho}}\left(\frac{A_i}{A_{0,i}}\right)^{1/4}, \quad W_{3,i} = \frac{\Gamma_i}{A_i}, \tag{3}$$

where under physiological conditions, i.e.,

$$\frac{Q_i}{A_i} \ll v_c(A_i) = \sqrt{\frac{G_{0,i}}{2\rho}}\sqrt{\frac{A_i}{A_{0,i}}}, \tag{4}$$

it can be shown that $W_{1,i}$ is a backward and $W_{2,i}$ is a forward traveling wave. The propagation of $W_{3,i}$ depends on the sign of $Q_i$.

Based on the small displacement hypothesis $A_i \approx A_{0,i} = \pi R_{0,i}^2$ and the assumption that $G_{0,i}$ and $A_{0,i}$ are constant along $z$, we linearize the non-linear transport equation system given by (1a), (1b) and (2) about the reference state $\left(A_{0,i}, 0, 0\right)$ [23]. The propagation of the oxygen concentration is carried out by a transport equation, whose velocity field is determined by the ratio of the flow rate and the section area $A_{0,i}$ [4] [8, Chapter 6]:

$$\frac{\partial p_i}{\partial t} + \frac{1}{C_i}\frac{\partial q_i}{\partial z} = 0, \quad z \in (0, l_i),\ t > 0, \tag{5a}$$

$$\frac{\partial q_i}{\partial t} + \frac{1}{L_i}\frac{\partial p_i}{\partial z} = -R_i \cdot q_i, \quad z \in (0, l_i),\ t > 0, \tag{5b}$$

$$\frac{\partial c_i}{\partial t} + \frac{\partial}{\partial z}\left(\frac{q_i \cdot c_i}{A_{0,i}}\right) = 0, \quad z \in (0, l_i),\ t > 0, \tag{5c}$$